HYDROGRAPHISCHE NACHRICHTEN

Journal of Applied Hydrography 06/2023 HN 125

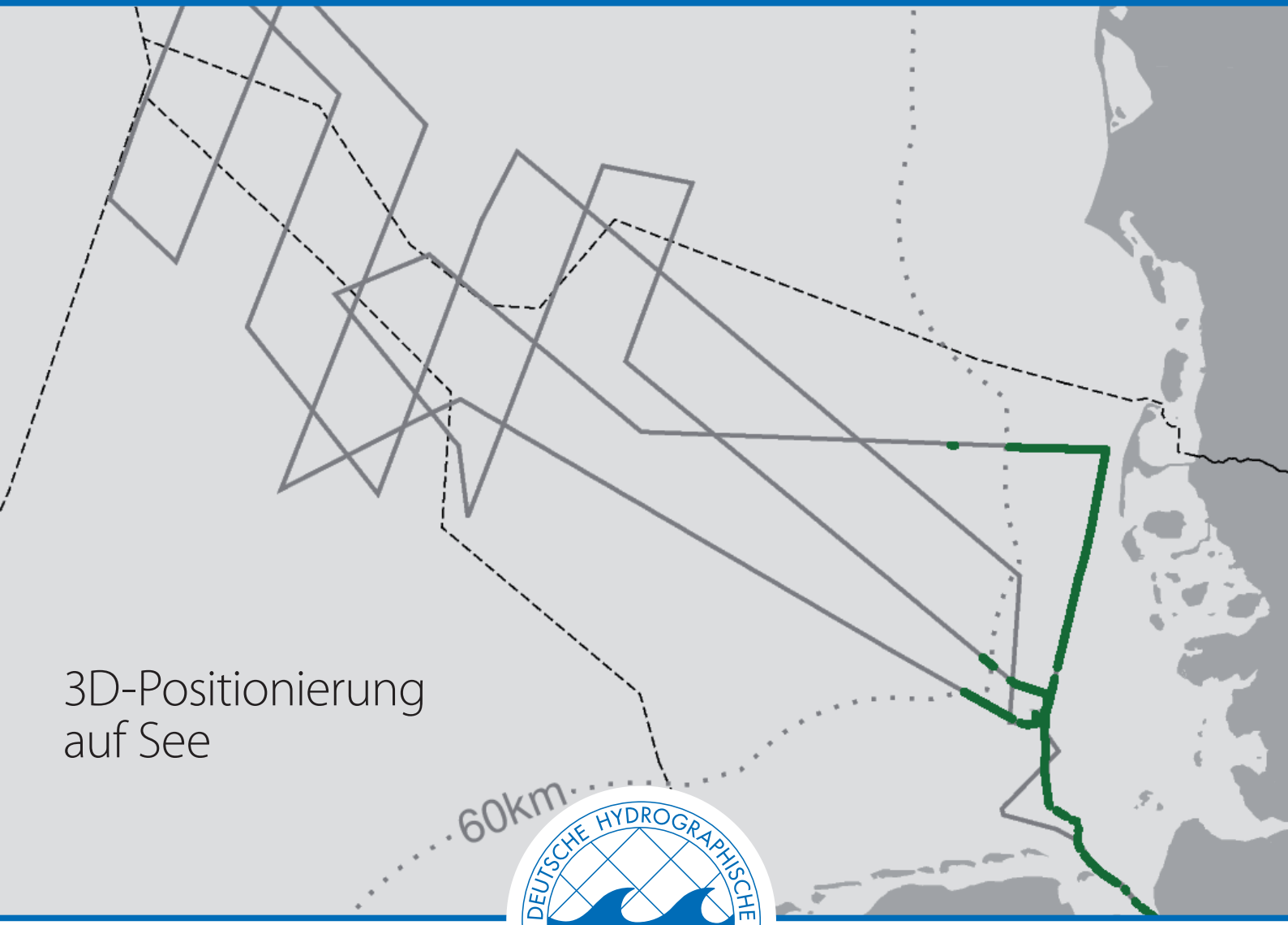

3D-Positionierung auf See

DEUTSCHE HYDROGRAPHISCHE GESELLSCHAFT e.V. DHyG

DOI: 10.23784/HN125-01

Robotic photogrammetric underwater inspection of hydropower plants

An article by MANUELA AMMANN

Hydropower is the most important domestic source of renewable energy in Switzerland, accounting for around 57 % of domestic electricity production. The high intensity usage of hydropower plants results in high costs for regular maintenance and inspection, which are currently carried out through manual inspections by professional divers. The aim of this work was to develop a workflow for underwater photogrammetry with remotely operated vehicles (ROV) to supplement or replace these dangerous and expensive dives. A calibration frame was developed to provide a scale reference for the data collected during the inspection. With different acquisition missions, investigations on camera calibration and 3D reconstruction were performed. The reconstruction of underwater objects was successfully implemented. Well-distributed control points provide accurate results as a point cloud with a sub-centimetre accuracy at object distances of up to 6 metres. 80 % of the point cloud differ less than 1 centimetre from the reference scan.

underwater photogrammetry | 3D reconstruction | structure from motion | camera calibration | ROV
Unter-Wasser-Photogrammetrie | 3D-Rekonstruktion | Structure-from-motion | Kamerakalibrierung | ROV

Wasserkraft ist mit einem Anteil von rund 57 % an der Stromproduktion die wichtigste inländische Quelle für erneuerbare Energien in der Schweiz. Die hohe Nutzungsintensität von Wasserkraftwerken führt zu hohen Kosten für die regelmäßige Wartung und Inspektion, die derzeit durch manuelle Inspektionen von professionellen Tauchern durchgeführt werden. Ziel dieser Arbeit war es, einen Arbeitsablauf für die Unter-Wasser-Photogrammetrie mit ferngesteuerten Fahrzeugen (ROV) zu entwickeln, um die gefährlichen und teuren Tauchgänge zu ergänzen oder zu ersetzen. Es wurde ein Kalibrierungsrahmen entwickelt, um einen Maßstabsbezug für die während der Inspektion erfassten Daten zu schaffen. Mit verschiedenen Erfassungsmissionen wurden Untersuchungen zur Kamerakalibrierung und 3D-Rekonstruktion durchgeführt. Die Rekonstruktion von Unter-Wasser-Objekten wurde erfolgreich umgesetzt. Gut verteilte Passpunkte liefern genaue Ergebnisse als Punktwolke mit einer Sub-Zentimeter-Genauigkeit bei Objektabständen von bis zu 6 Metern. 80 % der Punktwolke weichen weniger als 1 Zentimeter vom Referenzscan ab.

Author
Manuela Ammann is research assistant at FHNW Universities of Applied Sciences and Arts Northwestern Switzerland in Muttenz.

manuela.ammann@fhnw.ch

1 Introduction

Due to the topography and considerable average rainfall, Switzerland offers ideal conditions for the use of hydroelectric power. With around 57 % of domestic electricity production, hydropower is our most important domestic source of renewable energy (BFE 2022). A major challenge associated with hydropower generation and storage is the high intensity of the plants, resulting in high costs for regular maintenance and inspection of these plants. Current underwater inspections of hydropower plants in rivers can be dangerous and expensive, as manual inspections by professional divers are necessary. The aim of this project in cooperation with Axpo Power AG and Schuck Consulting was the development and verification of a novel workflow for 3D mapping based on an ROV-based underwater structure-from-motion process.

2 Related work

3D reconstruction is used in various fields. The image-based reconstruction of in air objects is already well researched. Various applications exist, where 3D underwater reconstruction is used, for example monitoring marine ecosystems (Neyer, Nocerino and Gruen 2018), mapping archaeological heritage (Bruno et al. 2015) and underwater construction (Chemisky et al. 2021), etc.

Underwater reconstruction applications with optical systems require images from a short distance, whereby a large number of images is needed to create complete 3D scenes (Chemisky et al. 2021). For true-to-scale 3D reconstructions, a scaling factor is applied leveraging control points with local or global coordinates, scale bars or stereo camera configurations. The accuracy of the 3D model mainly depends on the quality of the images (contrast, sharpness, exposure), the environ-

mental conditions (visibility, particles in the field of view) and the scene (heterogeneity of texture, moving objects). Furthermore, parameters such as the scaling method or the camera calibration influence the accuracy of the reconstruction (Chemisky et al. 2021).

Comprehensive calibration is essential, when accuracy is important and especially when the measured object has a 3D surface (Shortis 2019). There are different approaches to calibrate the camera, e.g. using a scale bar (Aragón et al. 2018), reference tape measurements (McCarthy and Benjamin 2014), a target board or plane (Menna, Nocerino and Remondino 2017) or a geodetic network (Neyer, Nocerino and Gruen 2018).

3 Materials and methods

3.1 Materials

For this project a Sony Alpha 7 II (ILCE-7M2) (Sony Europe B.V. 2022) with a lens FE 28 mm F2 (SEL28F20) with a 75° FOV is used. The camera is placed in a Sony A7 II NG V.2 Series UW underwater camera housing kit with an 8" dome port from seafrog (seafrogs 2023). The housing is mounted underneath a BlueROV2 (Fig. 1), which is an underwater robot with open-source electronics and software (Blue Robotics Inc 2022). Because the camera housing is larger than what the payload kit allows, the height was extended by 3D printed plates (Fig. 1, right). The ROV is manually steered on an external computer via the ROV camera stream.

Fig. 1: ROV (left) and ROV with extended payload-kit and the camera (right)

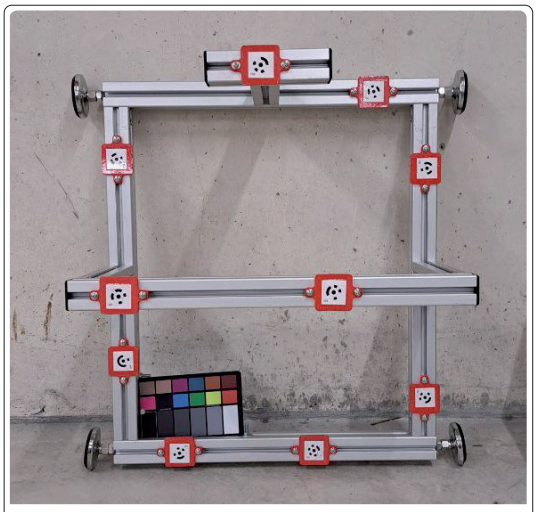

Fig. 2: Calibration frame with the colour chart in the bottom left

3.2 Calibration frame

A calibration frame made of aluminium (Fig. 2) was developed to perform a self-calibration during the 3D reconstruction. The objects of interest are captured by moving the ROV on an arc on different heights, due to the fixed mounting of the camera, which allows horizontal image capturing only. Multiple exposures should ensure the redundancy of the images.

3.3 Study areas and data acquisition

To capture test data three different study areas were evaluated. The indoor swimming pool in Muttenz was used for test capturing in clear water. Furthermore, the water lock (Fig. 3 and Fig. 4) was

Fig. 3: The hydropower plant in Eglisau: The water lock (orange) and the water filter (blue) in the inlet basin

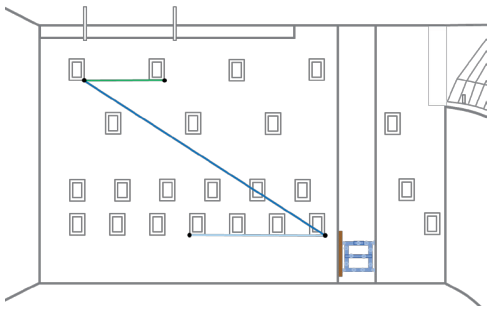

Fig. 4: Sketch of the water lock wall, the mounted calibration frame (blue object) and the measured lines for comparison: line 1 (green), line 2 (dark blue) and line 3 (light blue)

used for the capturing with a reference measurement, which were performed with the laser scanner. By filling the lock, different water levels can be set, simulating different depths (1 to 10 m) of acquisition. And finally, a water filter in the water (Fig. 3) was used to have a real object.

The focus of the camera could not be set manually due to the camera trigger software available with the test system. A summary of the image acquisition at the hydropower station in Eglisau can be found in Table 1.

Date	Environment	Places	Images	Distance	Depth
19.12.2022	In air	Indoor swimming pool	57	1.5 to 2 m	–
19.12.2022	In pool	Indoor swimming pool	202	2 m	2 m
30.11.2022	In river	Water lock	271	0.1 to 2 m	1, 3, 5, 7 and 10 m
20.01.2023	In river	Water lock	1594	0.1 to 2 m	0.5 to 10 m
20.01.2023	In river	Water lock	359	0.1 to 2 m	0.5 to 5 m

Table 1: Summary of the image based acquisition

Method	White balanced images	f	x_0	y_0	K_1	K_2	K_3	K_4	P_1	P_2	B_1	B_2
1	–	×	×	×	×	×	×	–	×	×	–	–
2	×	×	×	×	×	×	×	–	×	×	–	–
3	–	×	×	×	×	×	×	×	×	×	×	×

Table 2: Overview calibration methods

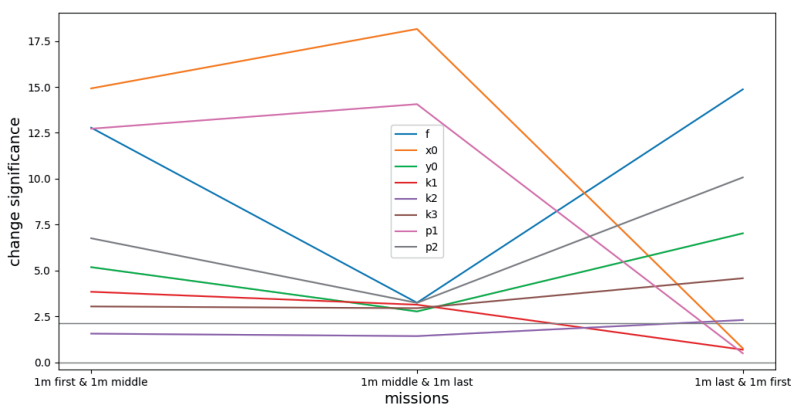

Fig. 5: Significant change of the first, middle & last part with method 1

For reference measurements, a Leica RTC360 laser scanner was used to create a dense and very accurate scan of the empty water lock with a 3D point accuracy of approximately 2.8 mm at 20 m and a Leica TS60 total station was used to determine control points for referencing in a local coordinate system with a 3D point accuracy of approximately 2.25 mm at 20 m.

3.4 Camera calibration

The camera was calibrated in Agisoft Metashape (Agisoft LLC 2022) conducting a self-calibration. The standard frame camera model of Metashape with Brown Distortion Model was used (Brown 1971).

The parameters focal length (f), principal point offset (x_0 and y_0), the radial distortion coefficients (K_1 to K_4), the tangential distortion coefficients (P_1 and P_2) and the affinity and non-orthogonality coefficients (B_1 and B_2) were determined. Different parameter sets were examined by three methods (Table 2) with original or pre-processed white balanced images. The values are statistically tested using the Student T distribution as in Harvey and Shortis (1998).

3.5 3D reconstruction

For 3D reconstruction, a dense point cloud was computed in Metashape with the self-calibrated cameras. The resulting point cloud of the water lock was compared to the reference scan using the plugin *M3C2* in CloudCompare (2023). Furthermore, the scale was controlled by three reference lines (Fig. 4) in the water lock.

For the point cloud of the water filter no reference data was available. To assess the quality of this mission, a cylinder is fitted into the data using the tool *Best Cylinder* in Cyclone 3DR (Leica Geosystems 2023) from Leica and the diameter is compared with the nominal value of the manufacturer (32.39 cm).

4 Results

4.1 Camera calibration

All missions and methods varied significantly, hence, a mission with calibration method 1 was divided into three parts of 20 images each. For these parts the calibration was recalculated. Fig. 5 shows that even in one mission the camera results in significantly different parameters.

4.2 3D reconstruction

The processed point clouds of the water lock were compared to the reference scan for each calibration method. Fig. 6 shows a close-up of the histograms of the deviation between 3D reconstruction and reference scan. 80 % of the points in the point cloud of method 1, 78 % of method 2 and 80 % of method 3 differ less than 1 cm.

The reference lines show similar results (Table 3). The largest differences occur at the shortest reference distance, which is slightly extrapolating and has less image overlap. One mission (based frame at last column) shows greater differences with an average of 3.6 cm. The mission is orientated based on the calibration frame only and thus the lines were extrapolated.

The reconstruction of the water filter (Fig. 7) is referenced based on the calibration frame and results in a very dense point cloud (point distance up to 0.3 mm). However, the reconstructed point cloud has missing parts.

The *Best Cylinder* tool was applied to the points of the pipe and results in a cylinder with a diameter of 33.12 cm (Fig. 8). Therefore, a difference of 0.73 cm to the nominal diameter resulted.

5 Discussion

The camera calibrations of the different missions, as well as the different calibration methods, show a significant variability (Fig. 5). Possible explanations are the instable mounting in the water housing and the autofocus.

However, as discussed by Luhmann (2018), if the 3D measurements in object space later turns out sufficiently accurate, the corresponding camera calibration is also sufficient. Hence, the processing of the 3D reconstruction can successfully be carried out and investigated.

For each method, a point cloud was reconstructed. There are no major differences between the calibration methods (Fig. 6). Only the point clouds from method 2 are slightly more widely distributed than those from the other methods. The white balanced images do not improve the results of these missions. Since method 3 uses more parameters, there are more uncertainties possible. Therefore, it is recommended to use method 1.

The largest deviations of the distances were found in the extrapolated areas of the water lock, while areas within the control points showed only a deviation of 1 cm. The results from the mission, which orientation is based on the calibration frame, revealed even larger deviations.

The water filter could be reconstructed as a 3D point cloud (Fig. 7). There are certain holes in the point cloud which are probably from a small image overlap, the fixed acquisition angle of the

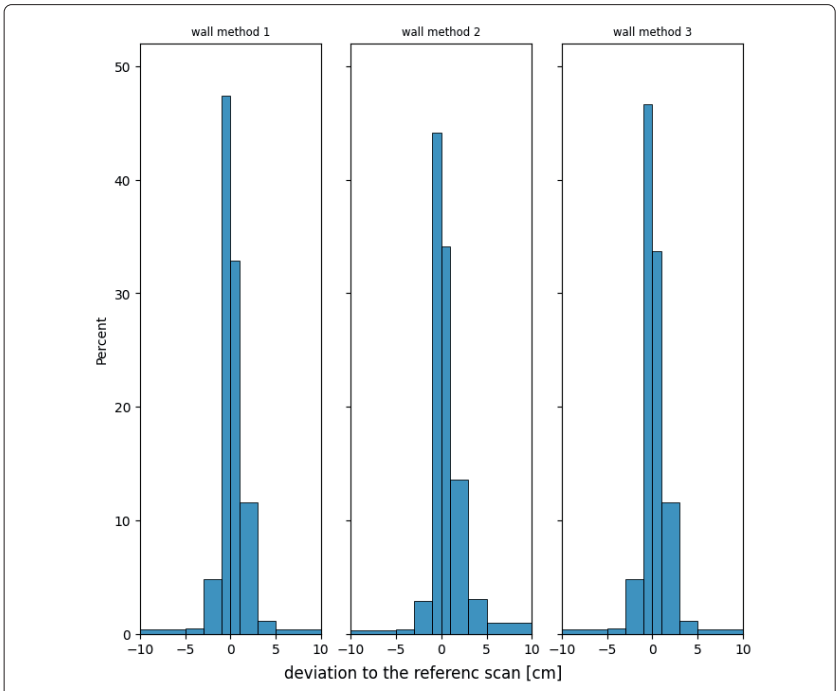

Fig. 6: Deviation per calibration method of the point cloud to the reference scan (close up)

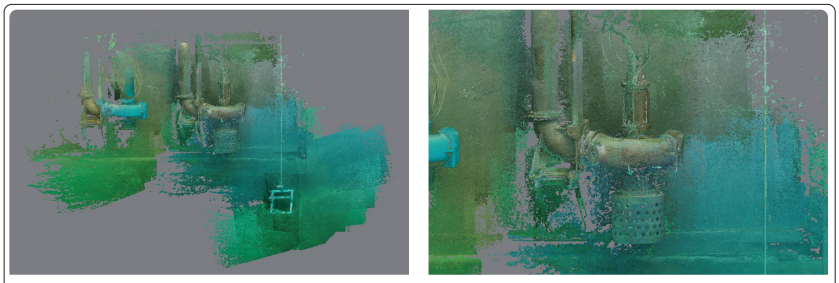

Fig. 7: Point cloud of the water filter (left) and a close up (right)

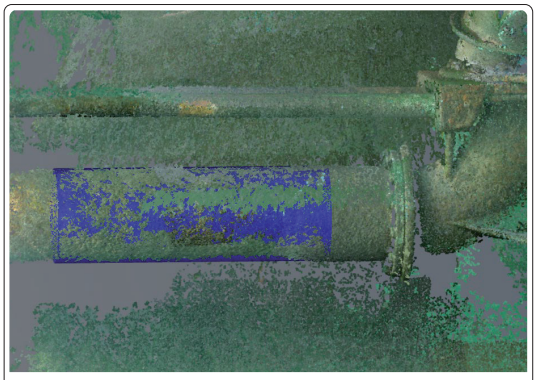

Fig. 8: Calculated cylinder for the pipe in the point cloud of the water filter (figure rotated by 90°)

	Reference scan	TS60 points	Photogrammetric reconstruction						Reconstruction – based frame	
			Method 1	Method 2	Method 3	Δ method 1	Δ method 2	Δ method 3	Method 1	Δ method 1
Line 1	3.722	3.725	3.709 m	3.713 m	3.708 m	**1.6 cm**	**1.2 cm**	**1.7 cm**	3.684 m	4.1 cm
Line 2	5.835	–	5.838 m	5.835 m	5.836 m	0.3 cm	0.0 cm	0.1 cm	5.825 m	1.0 cm
Line 3	12.764	12.764	12.766 m	12.768 m	12.766 m	0.2 cm	0.4 cm	0.2 cm	12.706 m	5.8 cm
						Ø 0.7 cm	Ø 0.6 cm	Ø 0.7 cm		Ø 3.6 cm

Table 3: Comparison of line measurements in the point cloud and the reference scan

camera or the difficulties with the access of the object. The tool *Best Cylinder* fits a cylinder in the point cloud. Despite the large extrapolation, as is referenced based on the calibration frame, the difference is 0.73 cm to the nominal diameter (Fig. 8).

6 Conclusion and outlook

The photogrammetric reconstruction of underwater objects was successfully implemented with the current set-up. Thanks to the calibration frame and additional control points, true-to-scale and very dense point clouds can be reconstructed, which can be used for further purposes. With well distributed control points, accuracies of sub-centimetres at distances of up to 6 m and 80 % of the points within a deviation of ±1 cm can be achieved.

While survey areas framed by control points showed less deviation than 1 cm, the largest deviations of the distances were found in the extrapolated areas of the water lock. More calibration frames or scale positioning in the area could potentially reduce the distortion over larger distances. Future research should be in this field.

The calibration results of the different missions and methods show a significant variability. Further investigations with improved camera mounting and better camera control are needed to determine the cause of these variations. A good camera calibration could improve the accuracy of extrapolation.

The water filter was successfully reconstructed as a 3D point cloud, however, there are some limitations with this set-up as the point cloud has holes. This can be attributed to low image overlap, the fixed acquisition angle of the camera or the lack of access. The tool *Best Cylinder* could successfully fit a cylinder into the point cloud, despite the large extrapolation. //

References

Agisoft LLC (2022): Agisoft Metashape. www.agisoft.com/ (accessed 10 October 2022)

Aragón, Enrique; Sebastia Munar; Javier Rodríguez; Kotaro Yamafune (2018): Underwater photogrammetric monitoring techniques for mid-depth shipwrecks. Journal of Cultural Heritage, DOI: 10.1016/j.culher.2017.12.007

BFE (2022): Wasserkraft. Bundesamt für Energie; www.bfe.admin.ch/bfe/de/home/versorgung/erneuerbare-energien/wasserkraft.html (accessed 3 October 2022)

Blue Robotics Inc (2022): BlueROV2. Blue Robotics; https://bluerobotics.com/store/rov/bluerov2/ (accessed 26 September 2022)

Brown, Duane C. (1971): Close-range camera calibration. Photogrammetric Engineering, No. 37, pp. 855–866

Bruno, Fabio; Antonio Lagudi; Alessandro Gallo; Maurizio Muzzupappa; Barbara Davidde Petriaggi; Salvatore Passaro (2015): 3D Documentation of Archaeological Remains in the Underwater Park of Baiae. The International Archives of the Photogrammetry, Remote Sensing and Spatial Information Sciences, DOI: 10.5194/isprsarchives-XL-5-W5-41-2015

Chemisky, Bertrand; Fabio Menna; Erica Nocerino; Pierre Drap (2021): Underwater Survey for Oil and Gas Industry: A Review of Close Range Optical Methods. Remote Sensing, DOI: 10.3390/rs13142789

CloudCompare (2023): CloudCompare – Open Source project. www.cloudcompare.org (accessed 1 February 2023)

Harvey, Euan Sinclair; Mark R. Shortis (1998): Calibration stability of an underwater stereo-video system: implications for measurement accuracy and precision. Marine Technology Society Journal, No. 32, pp. 3–17

Leica Geosystems (2023): Leica Cyclone 3DR. https://leica-geosystems.com/de-CH/products/laser-scanners/software/leica-cyclone/leica-cyclone-3dr (accessed 1 February 2023)

Luhmann, Thomas (2018): Nahbereichsphotogrammetrie: Grundlagen – Methoden – Beispiele. 4., neu bearbeitete und erweiterte Auflage. Wichmann-Verlag

McCarthy, John; Jonathan Benjamin (2014): Multi-image Photogrammetry for Underwater Archaeological Site Recording: An Accessible, Diver-Based Approach. Journal of Maritime Archaeology, DOI: 10.1007/s11457-014-9127-7

Menna, Fabio; Erica Nocerino; Fabio Remondino (2017): Flat Versus Hemispherical Dome Ports in Underwater Photogrammetry. The International Archives of the Photogrammetry, Remote Sensing and Spatial Information Sciences, DOI: 10.5194/isprs-archives-XLII-2-W3-481-2017

Neyer, Fabian; Erica Nocerino; Armin Gruen (2018): Monitoring Coral Growth - Comparing Underwater Photogrammetry and Geodetic Control Network. The International Archives of the Photogrammetry, Remote Sensing and Spatial Information Sciences, DOI: 10.5194/isprs-archives-XLII-2-759-2018

seafrogs (2023): Sony A7 II NG V.2 Series UW camera housing kit with 8" Dome port. seafrogs, https://seafrogs.com.hk/ (accessed 17 January 2023)

Shortis, Mark (2019): Camera Calibration Techniques for Accurate Measurement Underwater. In: 3D Recording and Interpretation for Maritime Archaeology. Coastal Research Library, Springer International Publishing, DOI: 10.1007/978-3-030-03635-5_2

Sony Europe B.V. (2022): Sony Alpha 7 II. Sony, www.sony.ch/de/electronics/wechselobjektivkameras/ilce-7m2-body-kit (accessed 17 January 2023)